



1 **Potentially Bioavailable Iron Delivery by Iceberg-hosted Sediments and Atmospheric Dust**  
2 **to the Polar Oceans**

3 **Rob Raiswell<sup>1</sup>, Jon R. Hawkings<sup>2</sup>, Liane G. Benning<sup>1,3</sup>, Alex R. Baker<sup>4</sup>, Ros Death<sup>2</sup>, Samuel**  
4 **Albani<sup>5</sup>, Natalie Mahowald<sup>5</sup>, Mike D. Krom<sup>1,6</sup>, Simon W. Poulton<sup>1</sup>, Jemma Wadham<sup>2</sup> and**  
5 **Martyn Tranter<sup>2</sup>.**

6 <sup>1</sup>Cohen Biogeochemistry Laboratory, School of Earth and Environment, University of Leeds,  
7 Leeds LS2 9JT, UK.

8 <sup>2</sup> Bristol Glaciology Centre, School of Geographical Sciences, University of Bristol, Bristol BS8  
9 1SS, UK.

10 <sup>3</sup> GFZ, German Research Centre for Geosciences, Telegrafenberg, D-11473 Potsdam, Germany.

11 <sup>4</sup>Laboratory for Global Marine and Atmospheric Chemistry, School of Environmental Sciences,  
12 University of East Anglia, Norwich NR4 7TJ, UK.

13 <sup>5</sup>Department of Earth and Atmospheric Sciences, Cornell University, Ithaca, New York, USA.

14 <sup>6</sup>Department of Marine Biology, Haifa University, Haifa, Israel.

15 RR Corresponding Author: email r.raiswell@see.leeds.ac.uk

16

17 **Abstract:** Iceberg-hosted sediments and atmospheric dusts transport potentially bioavailable iron  
18 to the Arctic and Southern Oceans as nanoparticulate ferrihydrite (the most soluble and  
19 potentially bioavailable iron (oxyhydr)oxide mineral). A suite of more than 50 iceberg-hosted  
20 sediments contain a mean content of 0.076 wt. % Fe as nanoparticulate ferrihydrite, which  
21 produces iceberg-hosted Fe fluxes ranging from 1.4-11 and 3.2-25 Gmoles yr<sup>-1</sup> to the Arctic and  
22 Southern Oceans respectively. Atmospheric dust contains a mean nanoparticulate ferrihydrite Fe  
23 content of 0.038 wt. % (corresponding to a fractional solubility of ~ 1%) and delivers much  
24 smaller Fe fluxes (0.02-0.07 Gmoles yr<sup>-1</sup> to the Arctic Ocean and 0.0-0.02 Gmoles yr<sup>-1</sup> to the  
25 Southern Ocean). New dust flux data show that most atmospheric dust is delivered to sea ice  
26 where exposure to melting/re-freezing cycles may enhance fractional solubility, and thus fluxes,  
27 by a factor of approximately 2.5. Improved estimates for these particulate sources require  
28 additional data for the sediment content of icebergs and samples of atmospheric dust delivered to  
29 the polar regions.

30



## 31 1. Introduction

32 Iron (Fe) is an essential limiting nutrient for phytoplankton. Its supply exerts a significant  
33 impact on marine productivity with important implications for the carbon cycle and climate  
34 change (Mackenzie and Andersson, 2013). Quantifying Fe sources to the oceans, especially  
35 those that may be influenced by climate change, is therefore critical. Global Fe cycles commonly  
36 recognise important supplies of dissolved Fe (dFe, <math><0.2</math> or <math>0.45\mu\text{m}</math>) from atmospheric dust,  
37 continental shelf sediments and hydrothermal activity (e.g., Breitbart et al., 2010).  
38 Contributions from hydrothermal activity and shelf sediments are based on estimates and/or  
39 measurements of dFe (see Tagliabue et al., 2010; Dale et al., 2015) but quantifying dFe  
40 contributions from atmospheric dusts requires an estimate of the solubility of iron. Estimating the  
41 solubility of Fe in particulates is particularly important in understanding the Fe cycle in the polar  
42 oceans where the iceberg-hosted sediments are a source of bioavailable Fe (Smith et al., 2007;  
43 Raiswell et al., 2008; Hawkings et al., 2014; Luis et al., 2016).

44 The Southern Ocean (SO) is the largest HNLC (High Nutrient-Low Chlorophyll) area  
45 where productivity is limited by the delivery of Fe (e.g. Moore et al., 2013). Recent modelling  
46 studies in the SO have focussed on understanding the factors which control spatial variations in  
47 productivity but reach different conclusions due to different representations of the Fe cycle and  
48 different assumptions as to Fe solubility and scavenging. For example; Tagliabue et al. (2009)  
49 modelled measurements of dFe derived from atmospheric dust and shelf sediments. Atmospheric  
50 dusts entering seawater were assumed to have a fractional solubility (soluble Fe expressed as a  
51 percentage of total Fe) of 0.5% with continued slower dissolution during sinking occurring at a  
52 rate of 0.0002% per day. Overall sediments were more important than atmospheric dust,  
53 although dust supplies dominated in some regions depending on the model assumptions used.  
54 Lancelot et al. (2009) modelled dFe supplies from atmospheric dust, iceberg melt and shelf  
55 sediments. Sediments were the major source, iceberg melt was of lesser significance and  
56 atmospheric dust (assumed to have fractional solubility of 2%) had little influence. The models  
57 gave good agreement with patterns of phytoplankton growth but large uncertainties were  
58 acknowledged in the magnitude of these sources. Boyd et al. (2012) compared biological  
59 utilisation patterns using four mechanisms of Fe supply (vertical diffusivity in sea ice free areas,  
60 iceberg melt, atmospheric dust and shelf sediments) that were found to have substantial areal



61 extent. Phytoplankton Fe utilisation was highest in regions supplied by Patagonian dust (using  
62 fractional solubilities varying from 1-10% Fe) and, to a lesser extent shelf sediments. Wadley et  
63 al. (2014) compared the relative magnitudes and variations in supply of dFe from melting  
64 icebergs, shelf sediments and atmospheric dust. Sediments were again shown to be the most  
65 important source but considerable uncertainty was noted over the flux of Fe from iceberg-hosted  
66 sediments. Death et al. (2014) considered a range of sources that included iceberg-hosted  
67 sediments and atmospheric dust and found that modelled productivity was significantly enhanced  
68 in areas receiving iceberg-hosted sediments and subglacial melt compared to the productivity  
69 arising from atmospheric dust (assumed fractional solubility of 2%). However the contribution  
70 from iceberg-hosted sediments was based on a suite of only six samples (Raiswell et al., 2008)  
71 that contained 0.15 wt. % Fe as ferrihydrite.

72 These studies show that SO models produce significant differences in the relative  
73 magnitudes of the different Fe sources which complicate attempts to isolate overlapping  
74 contributions. For example Tagliabue et al. (2015) shows that global dust fluxes of dFe range  
75 from 1-30 Gmoles yr<sup>-1</sup> between different models. Few studies also count for iceberg sources of  
76 Fe (see Tagliabue et al., 2015; Table 1), the importance of which may be particularly sensitive to  
77 climate change. Climate change is driving increased loss of ice from ice shelves in the Antarctic  
78 Peninsula (Vaughan, 2006; Rignot et al., 2011) and ice-shelf shrinkage has also been reported  
79 from other areas in Antarctica (Pritchard et al., 2012; Depoorter et al., 2013; Luis et al., 2016).  
80 Ice shelf losses increase the delivery of potentially bioavailable Fe by iceberg-hosted sediments.  
81 Iceberg-hosted sediment data are sparse but current estimates indicate Fe delivery appears to  
82 exceed meltwater delivery to the SO by at least an order of magnitude (Hawkings et al., 2014).

83 Increases in iceberg-hosted sediment delivery are also likely in the Arctic Ocean (AO).  
84 A relatively high proportion of primary production occurs on the AO shelves (Pabi et al., 2008)  
85 where ice-free areas experience intense phytoplankton blooms due to favourable light and  
86 nutrient conditions. Nitrate appears to be the primary limiting nutrient otherwise Fe and/or light  
87 become limiting (Popova et al., 2010). Hawkings et al. (2014) have estimated Fe delivery by  
88 meltwaters from the Greenland Ice Sheet but no data are available for Fe delivery from iceberg-  
89 hosted sediments, although marine-terminating glaciers in the AO are likely to respond to



90 climate change, as in the SO, by producing more icebergs (Bamber et al., 2012) and increasing  
91 sediment Fe delivery.

92 Modelling the polar Fe cycles and assessing the impact of climate change requires an  
93 improved estimate of the Fe currently released from the particulates present as iceberg-hosted  
94 sediments and atmospheric dust. There is a substantial disagreement as to the strength of  
95 different sources and reducing their uncertainty is important (Tagliabue et al., 2015). This  
96 contribution presents new data for potentially bioavailable Fe from iceberg-hosted sediments and  
97 atmospheric dust and also shows how ice transport and storage may influence Fe delivery to the  
98 polar regions. The AO and the SO differ in several important respects. The AO receives more  
99 atmospheric combustion products (Luo et al., 2008), has a proportionately smaller area of winter  
100 ice (see later) and is also being disproportionately affected by global warming (IPCC, 2013).  
101 Changes in Fe delivery to the SO may influence productivity but this is unlikely in the AO where  
102 there is no evidence for Fe limitation (except perhaps in summer in the Irminger Basin;  
103 Nielsdottir et al., 2009).

104 The Fe budgets for the AO use the area  $>60^{\circ}\text{N}$  (a larger area than that  $>66^{\circ}33/39'\text{N}$  which  
105 is conventionally used to define the Arctic Ocean; Pabi et al., 2008) and the SO budget is based  
106 on the area  $>60^{\circ}\text{S}$ . The  $60^{\circ}\text{S}$  latitude lies close to the Antarctic Polar Front (the boundary  
107 between cold Antarctic waters and warmer sub-Antarctic waters), which runs clockwise from  
108  $140^{\circ}\text{E}$  to  $60^{\circ}\text{W}$ , beyond which the front moves out to  $48^{\circ}\text{S}$  (Moore et al., 1999). Our new flux  
109 estimates are based on measurements of ferrihydrite Fe which are determined by the source and  
110 mode of delivery and have a fundamental influence on bioavailability. We are concerned only  
111 with glacial and atmospheric particulate sources that can be significantly influenced by terrestrial  
112 and/or transport processes prior to entry into seawater. The fate of these sources on entering  
113 seawater and their spatial variations are outside this focus although our data may inform these  
114 research areas.

## 115 **2. Methodology**

### 116 **2.1 Ice-hosted Sediment Sampling**

117 Over 60 sediment samples have been collected from icebergs and glaciers at 15 different  
118 Arctic and Antarctic locations (Table S1). Data have previously been reported for only 15 of



119 these samples (from 7 localities, see Table S1) and thus the new samples provide a significant  
120 expansion of the existing data and now represent a substantial database for ice-hosted sediments.  
121 A set of 41 new iceberg samples were collected from floating icebergs with sediment-bearing  
122 layers present in dense, clear blue ice indicating compressed glacier ice rather than accreted  
123 frozen seawater. An additional suite of 9 new glacial ice samples was collected from sediment-  
124 rich bands in the main body of glaciers (i.e. land-based ice not icebergs). These samples  
125 represent basal ice which has been in contact with the ice-rock interface.

126 Samples were collected with a clean ice axe, geological hammer or chisel. The outer  
127 layers of ice that might be contaminated were allowed to melt and drain away before the  
128 remaining ice was transferred into a new polyethylene bag and allowed to melt. Some loss of  
129 dissolved Fe by adsorption or the precipitation of (oxyhydr)oxides during melting is possible  
130 (Conway et al., 2015) but the presence of organic complexes (see later) can stabilise dissolved  
131 Fe. In any event, melt dFe concentrations are too low (Hawkings et al., 2014) to produce any  
132 significant increase in sediment Fe contents. Sediment samples were collected as soon as melting  
133 was complete by filtration through a Whatman 542 (2.7  $\mu\text{m}$  pore diameter) filter paper or  
134 through a 0.4/0.45  $\mu\text{m}$  membrane filter (Table S3). There is a significant difference in the size  
135 fractions produced by filtration through 2.7  $\mu\text{m}$  and 0.4/0.45  $\mu\text{m}$  but the filtered iceberg sediment  
136 is dominated by coarser material and variations in the content and masses of the fraction passing  
137 through the different filters seem to be too small to produce significant differences in our  
138 extractable Fe contents, at least compared to the variations between different samples (see later,  
139 Tables 3 and S3). Small pebbles and grit (> 1mm diameter) were removed and the remaining  
140 material gently disaggregated but not crushed. Any further separations are as described below.

## 141 2.2 Atmospheric Dust Samples.

142 A suite of 15 atmospheric dust samples (Table S2) have been analysed by the same  
143 extraction techniques used for the iceberg and glacial samples to ensure data comparability.  
144 Seven new samples were collected during a cruise through the eastern tropical Atlantic and into  
145 the Sea of Marmara (Baker et al., 2006). These aerosol samples were collected using high  
146 volume (1  $\text{m}^3 \text{min}^{-1}$ ) aerosol samplers onto single acid-washed Whatman 41 filters (pore size 20  
147  $\mu\text{m}$ ; see Baker et al., 2006). Three new samples of dry deposition were collected from a clean  
148 window in Southern Patagonia and two new samples of dry deposition were collected from the



149 Eastern Mediterranean; one from a dust collector located in Crete and the other from deposition  
150 on to a clean glass surface at Rosh Pina, Israel. (Table S2). Relevant data from the literature  
151 (Table S2) are also included for 3 additional dry deposition samples from the Eastern  
152 Mediterranean and China (Table S2).

153

### 154 2.3 Analytical Methodology

155 Each sample of air-dried sediment was treated for 24 hours by an ascorbic acid solution  
156 buffered at pH 7.5. The extractant was a deoxygenated solution of 0.17M sodium citrate and  
157 0.6M sodium bicarbonate to which ascorbic acid was added to produce a concentration of  
158 0.057M. Approximately 10-40 mg of sample were mixed with 10 ml of the ascorbate solution,  
159 shaken for 24 hrs at room temperature and then filtered through a 0.45  $\mu\text{m}$  cellulose nitrate  
160 membrane filter (Kostka and Luther, 1994; Hyacinthe and Van Cappellen, 2004; Raiswell et al.,  
161 2010). The Fe removed by ascorbic acid is hereafter termed FeA and reported as dry wt. %. This  
162 technique quantitatively removes the Fe from fresh 2-line ferrihydrite and partially dissolves the  
163 Fe from aged 2-line and 6-line ferrihydrite and schwertmannite with negligible effects on other  
164 Fe (oxyhydr)oxides or clay minerals (Raiswell et al., 2010). The measurement of nanoparticulate  
165 ferrihydrite is important because this mineral phase is directly or indirectly bioavailable (Wells  
166 et al., 1983; Rich and Morel, 1990; Kuma and Matsunga, 1995; Nodwell and Price, 2001). The  
167 delivery of ferrihydrite to the open ocean thus has the potential to stimulate productivity in Fe-  
168 limited areas (Raiswell et al., 2008; Raiswell, 2011).

169 The residual sediment was treated for 2 hrs with a solution of 0.29M sodium dithionite in  
170 0.35M acetic acid and 0.2M sodium citrate, buffered at pH 4.8 (Raiswell, et al., 1994). Following  
171 the ascorbic acid extraction step, the dithionite extracts the remaining (oxyhydr)oxide Fe (aged  
172 ferrihydrite, goethite, lepidocrocite and hematite; Raiswell et al., 1994). Dithionite-soluble Fe is  
173 hereafter termed FeD and is reported as dry wt. %. Both the FeA and FeD extractant solutions  
174 were analysed for Fe either by Atomic Absorption Spectrometer with an air-acetylene flame or  
175 by spectrophotometry using ferrozine (Stookey, 1980). Replicate analysis of a river sediment  
176 internal laboratory standard gave analytical precisions of 3% for FeA and 10% for FeD using this  
177 sequential extraction. Errors associated with sampling glacial sediments are examined below.  
178 Blank corrections were negligible.



## 179 2.4 Approach

180 Estimates of the solubility of Fe in atmospheric dusts have utilised a variety of extraction  
181 techniques that attempt to simulate the complex reactions that may occur during cloud  
182 processing. Jickells and Spokes (2001) have summarised the dust extraction data and show that  
183 the estimates of fractional solubility range from 0.2 to 80%, depending on time, pH and the  
184 extractant (Baker and Croot, 2010). Few of these extractions have been fully calibrated against  
185 different Fe minerals. For example Baker et al. (2006) extracted Fe using ammonium acetate at  
186 pH 4.7 which dissolves negligible concentrations of Fe (oxyhydr)oxides but significant  
187 concentrations of Fe as carbonate (Poulton and Canfield, 2005). Chen and Siefert (2003)  
188 extracted Fe with a 0.5 mM formate-acetate buffer at pH 4.5 which was stated to dissolve Fe  
189 (oxyhydr)oxides (mineralogy unspecified). Our ascorbic acid extraction is more selective for  
190 ferrihydrite than the Baker et al. (2006) extraction but weaker than the Chen and Siefert (2003)  
191 extract (compared to which the ascorbic extract is at a higher pH, and is selective for  
192 ferrihydrite).

193 We recognise two particulate fractions (Raiswell and Canfield, 2012) that contain Fe  
194 (oxyhydr)oxide minerals (ferrihydrite, lepidocrocite, goethite and hematite), as described below.

195 (1) FeA reported as wt. % Fe that is extractable by ascorbic acid and which consists  
196 mainly of fresh, nanoparticulate ferrihydrite (Raiswell et al., 2011).

197 (2) FeD reported as wt. % Fe that is extractable by dithionite. Extraction of FeD  
198 following removal of FeA mainly dissolves residual, aged ferrihydrite plus  
199 lepidocrocite, goethite and hematite (Raiswell et al., 1994).

200 An important issue concerns the bioavailability of FeA and FeD. Experimental work  
201 suggests that some part of sediment Fe can support plankton growth (Smith et al. 2007; Sugie et  
202 al., 2013). Sediment Fe present as fresh ferrihydrite (the most soluble Fe (oxyhydr)oxide) is  
203 directly or indirectly bioavailable (see above) and is extracted as FeA. FeA mainly comprises  
204 nanoparticulate ferrihydrite but probably encompasses a range in bioavailabilities (Shaked and  
205 Lis, 2012) due to variations in the extent of aggregation and associations with organic matter  
206 (which may partially or wholly envelope Fe (oxyhydr)oxide minerals; Raiswell and Canfield,  
207 2012). We are concerned with Fe mineral reactivity at the point of delivery to seawater where



208 ferrihydrite measured as FeA is more labile than FeD (the dithionite-soluble (oxyhydr)oxides  
209 which are relatively stable and poorly bioavailable). However, Fe present as FeD may become  
210 partially bioavailable after delivery to seawater (for example by dissolution and grazing;  
211 Raiswell and Canfield, 2012; Shaked and Lis, 2012), but these complex interactions are outside  
212 the scope of the present contribution.

### 213 **3. Results and Interpretation**

#### 214 3.1 Reproducibility of Iceberg Sediment Sampling.

215 The collection of small samples from heterogeneous sediment with a range of grain sizes  
216 (clay up to sand-size and beyond) is difficult to do reproducibly. Our approach has been to  
217 examine the variability both within and between different size-fractions. Our previous practice  
218 (Raiswell et al., 2008) has been to remove only coarse material >1mm diameter, which might  
219 severely affect our ability to analyse sub-samples of 10-40 mg reproducibly. Table 1 compares  
220 the composition of different size fractions produced by sieving iceberg sediment (from  
221 Wallensbergfjorden, Svalbard) first to <1mm, then by taking two further replicate subsamples:  
222 one sieved to <250  $\mu\text{m}$  and the other to <63  $\mu\text{m}$ . Five replicates were analysed from each size  
223 fraction to give the means and standard deviations in Table 1.

224 A student's *t* test showed no significant differences between mean analyses of wt. % FeA  
225 in the three different size fractions. In general the wt. % FeA would be expected to be larger in  
226 the finer fractions, but the enrichment need not be large. A comparison of the FeA contents of  
227 the glacial flours studied by Hopwood et al. (2014) showed that <500  $\mu\text{m}$  fractions contained 40-  
228 130% of the FeA content of the <63  $\mu\text{m}$  fraction. Shaw et al. (2011) also found a rather similar  
229 wt % of FeA in the 63-125  $\mu\text{m}$  (0.038%) and 125-500 $\mu\text{m}$  (0.053%) fractions of iceberg  
230 sediment. Thus the finest fractions are not always large enough in mass, or have a high enough  
231 wt. % FeA, to produce substantial differences between the different size fractions. We next  
232 examined the sampling reproducibility using five different iceberg samples (K1-5) from  
233 Kongsfjord, Svalbard (see Table S3) that were sieved through 1mm with a replicate subsample  
234 then produced by sieving to <63  $\mu\text{m}$ . Table 2 shows the mean and standard deviation for 5  
235 replicate analyses of these iceberg samples sieved through <1 mm and compared to a single  
236 analysis of the <63  $\mu\text{m}$  fraction.





237 No consistent pattern emerged from the data presented in Table 2. Samples with low wt.  
238 % FeA values (K2 and K3) tended to show the most variation. However, the  $z$  test showed a high  
239 probability of there being no significant difference between the <1mm and <63  $\mu\text{m}$  samples for  
240 K1, K3 and K5 ( $p>5\%$ ) but a low probability ( $p<0.2\%$ ) that samples K2 and K4 were not  
241 significantly different. We conclude that our practice of removing only very coarse material by  
242 sieving through <1 mm provides a reasonable compromise that achieves good reproducibility  
243 (unless the wt. % FeA is less than 0.05%) in samples that are coarse enough to be representative  
244 of the sediments delivered by icebergs.

### 245 3.2. Ice-hosted Sediment Composition.

246 Table 3 summarises the wt. % FeA and FeD contents of the iceberg and glacier sediments  
247 and the mean and standard deviations of FeA and FeD. There are no significant differences  
248 between the compositions of the Arctic and Antarctic icebergs (if the outlying data for Weddell  
249 Sea IRD4 is ignored; see Table S3) and hence we are justified in presenting all the iceberg  
250 samples as a single group (Table 3).

251 The wt. % FeA and FeD data are log normally distributed and hence logarithmic means  
252 are used to calculate the mean values and the logarithmic standard deviations are used to derive  
253 the low and high values in Table 3. This approach produces a mean FeA content of 0.076 wt. %  
254 for the iceberg sediments and a range of 0.030% to 0.194%. These new values are based on more  
255 than 50 iceberg samples; thus this mean is more reliable than the earlier mean value of 0.15 wt.  
256 % FeA (based on only 6 samples from Raiswell et al., 2008) and the large number of samples  
257 also permit an estimate of the variation. A student's  $t$  test on the logarithmic data showed that  
258 the iceberg sediments are significantly higher ( $p<0.1\%$ ) than the logarithmic mean and standard  
259 deviation of the wt. % FeA contents of the sediments from glacial ice (mean 0.03%, range  
260 0.015% to 0.060%). The logarithmic mean and standard deviation of the values for wt. % FeD in  
261 Table 3 are also significantly higher ( $p<0.1\%$ ) in the icebergs (mean 0.377%, range 0.20% to  
262 0.715%) than in the sediments from glacial ice (mean 0.091% range 0.042% to 0.196%).

#### 263 3.2.1. Ice Processing Effects

264 The wt. % FeA and FeD contents of the iceberg sediments are significantly higher than  
265 the glacier-hosted sediments. The icebergs were not all derived from the land-based glaciers we



266 sampled, and part of the differences in FeA and FeD may result from mineralogical/geochemical  
267 variations in the glacial bedrock. An alternative explanation for the high wt. % FeA and FeD  
268 values is that iceberg sediments have undergone alteration during post-calving transport as  
269 temperature fluctuations induced melting and weathering. The slightly acidic pH (5.5-6.0) of  
270 snow and glacial icemelt (Meguro et al., 2004; Tranter and Jones, 2001) accompanied by the  
271 presence of extracellular polymeric substances (Lannuzel et al., 2014; Lutz et al., 2014) is able to  
272 accelerate the production of Fe (oxyhydr)oxides by weathering. Furthermore, Kim et al. (2010)  
273 has observed that UV radiation causes the photoreductive dissolution of Fe (oxyhydr)oxides  
274 (goethite, hematite) encased in ice to ferrous Fe. Photoreductive dissolution was significantly  
275 faster in ice than in aqueous solutions at pH 3.5 and was not influenced by the presence of  
276 electron donors. Acids are concentrated by several orders of magnitude at the ice-grain boundary  
277 due to freeze concentration effects and the resulting low pH (~1.5) further enhances  
278 photoreductive dissolution. Lin and Twinning (2012) have found elevated concentrations of  
279 ferrous Fe within 1 km of a melting iceberg in the Southern Ocean which they suggest could be  
280 derived by the photoreduction of FeA in melt pools. However, most ferrous Fe is likely to be  
281 rapidly re-oxidised and precipitated as (oxyhydr)oxide minerals once exposed to the atmosphere  
282 by melting, which dilutes the acids and increases pH. The redox recycling effects of repeated  
283 melting/freezing events are explored below, as they might apply to any sediments (including  
284 atmospheric dusts, see later) encased in ice.

285 Fig. 1 shows an idealised melting/freezing reaction scheme for any sediment in which Fe  
286 (oxyhydr)oxides are initially absent and that only contains silicate Fe. Dissolution is initiated in  
287 acidic snow melt where Fe is leached slowly by silicate dissolution (Step 1). Subsequent freezing  
288 (Step 2) halts dissolution and induces the precipitation and aggregation of Fe (oxyhydr)oxides as  
289 FeA and FeD. The transformation of ferrihydrite (FeA) to goethite/hematite (FeD) has a half-life  
290 of several years at  $T < 5^{\circ}\text{C}$  (Schwertmann et al., 2004; Brinza, 2010) and hence a proportion of  
291 FeA can be preserved over the life time of an iceberg. A new phase of melting (Step 3) causes  
292 the rapid dissolution or disaggregation of the newly formed FeA and FeD and also restarts the  
293 slow dissolution of silicate Fe, until renewed freezing (Step 4) again produces FeA and FeD in  
294 amounts that have now been increased by the Step 3 dissolution of silicate Fe. Provided there is  
295 insufficient time for the transformation of FeA to FeD to be completed then FeA and FeD will  
296 both accumulate at the expense of silicate Fe. A comparison of the mean FeA contents of the



297 glacial (0.03 wt. %) and iceberg (0.076 wt. %) sediments and their errors suggests that  
298 melting/freezing effects, hereafter termed ‘ice processing’, could increase FeA contents by factor  
299 of 2.5, assuming similar initial FeA contents. This data provides the first, semi-quantitative  
300 estimate of how deposition on to sea ice might enhance the FeA delivery from atmospheric dust.  
301 These changes may also be accompanied by other, poorly understood chemical mechanisms that  
302 may further enhance Fe delivery from sea ice (Vancoppenolle et al., 2013).

### 303 3.3 Iceberg-Hosted FeA Fluxes

304 The iceberg-hosted FeA flux (Table 4) is based on sediment encased in icebergs and  
305 excludes sediments associated with seasonal ice (see later). The solid ice discharge from  
306 Antarctica has been determined as  $1321 \pm 144 \text{ km}^3 \text{ yr}^{-1}$  by Depoorter et al. (2013) for the period  
307 1979-2010 and from Greenland as  $524 \pm 51 \text{ km}^3 \text{ yr}^{-1}$  for the period 1958-2010 by Bamber et al.  
308 (2012). Van Wychen et al. (2015) estimate that the contribution from other ice masses in Alaska,  
309 Svalbard, and the Russian and Canadian Arctic is  $34.4 \text{ km}^3 \text{ yr}^{-1}$  for which we assume a 10% error  
310 (roughly the same as for the Greenland flux). Hence the total ice loss from the Arctic is  $558 \pm 55$   
311  $\text{km}^3 \text{ yr}^{-1}$  and from the Antarctic is  $1321 \pm 144 \text{ km}^3 \text{ yr}^{-1}$ . Raiswell et al. (2006) and Death et al.  
312 (2014) point out that the sediment content of icebergs is poorly constrained but use a value of  $0.5$   
313  $\text{g litre}^{-1}$ , similar to the mean sediment content of river water. A value in the range  $0.6\text{--}1.2 \text{ g litre}^{-1}$   
314 has been inferred by Shaw et al. (2011) based on the sediment load needed to produce the excess  
315  $^{224}\text{Ra}$  activity in the vicinity of icebergs in the Weddell Sea. Here we use the conservative  
316 estimate of  $0.5 \text{ g litre}^{-1}$  of sediment but the asterix in Table 4 indicates that this value may be a  
317 significant source of error. The mean wt. % FeA content of icebergs is 0.076% with a variability  
318 of 0.030 to 0.194% (Table 3). Deriving the product of the ice mass loss, sediment load and FeA  
319 content (Table 4) shows that the flux of iceberg-hosted FeA to the AO ranges from 1.4 to 11  
320  $\text{Gmol yr}^{-1}$  with a mean of  $3.8 \text{ Gmol yr}^{-1}$ , and to the SO is 3.2 to 25  $\text{Gmol yr}^{-1}$  with a mean of  $9.0$   
321  $\text{Gmol yr}^{-1}$ . All flux values hereon are quoted to two significant figures. These ranges overlap  
322 because the same data have been used for the sediment and FeA contents of icebergs and because  
323 the iceberg discharge values to the AO and the SO only differ by a factor of 2.

### 324 3.4 Atmospheric Dust Composition



325 Mineralogy is a key factor in comparing particulate sources and use of the ascorbic acid  
326 extraction technique for the iceberg sediments and atmospheric dusts enables their ferrihydrite  
327 contents (as the most readily soluble and potentially bioavailable Fe mineral) to be compared.  
328 The atmospheric dust sample set is relatively small and mainly includes samples that are unlikely  
329 to be delivered to the polar regions although Patagonian dust is a possible source to the SO (e.g.  
330 Schulz et al., 2012). Our Patagonian dust sample set is small but a student's *t* test indicates that  
331 there are no significant differences in the concentrations of FeA and FeD between the Patagonian  
332 dusts and the other dusts analysed here. Consistent with this we note that the range of total Fe  
333 values (2.9 to 4.3 wt. %) for the Patagonian aeolian dusts analysed by Gaiero et al. (2007)  
334 overlaps the range in our dusts (2.8-4.5 wt.%; Table S4) and the mean value of 3.5 wt. %  
335 commonly assumed for atmospheric dust (e.g. Gao et al., 2003; Shi et al., 2012).

336 Our dust wt. % FeA contents are low (mean 0.038%, range 0.018 to 0.081%) and are  
337 comparable to the wt. % FeA contents of the sediments present in glacial ice, but significantly  
338 lower ( $p < 1\%$ ) than the iceberg-hosted sediments (Table 3). Assuming a dust total Fe (FeT) of 3.5  
339 wt. %, the range in wt. % FeA corresponds to a fractional solubility of  $\sim 1\%$ . This data provides a  
340 justification for the commonly used range of 1-2% (see earlier) which is known to be an arbitrary  
341 choice; Boyd et al., 2010). However our ascorbic acid fractional solubility data are difficult to  
342 compare with literature values because a wide range of extractions have been used, few of which  
343 have been calibrated against ferrihydrite (see earlier). Conway et al. (2015) have fractional  
344 solubility data based on the ratio between Fe extracted at pH 5.3 by meltwater and total Fe. A  
345 median value of 6% was found for dusts (deposited during the LGM on ice at Dome C, East  
346 Antarctica) that were high in total Fe (8%), possibly due to enrichment in smaller particles as a  
347 consequence of long range transport. Rather lower fractional solubility values ( $\sim 3\%$ ) were found  
348 at Berkner Island closer to the South American dust sources and these data are comparable to the  
349 FeA range of our dust data, assuming similar extraction behaviour.

350 Dust wt. % FeD values (mean 0.87%, range 0.43 to 1.76 %) are significantly higher ( $p$   
351  $< 0.1\%$ ) than in both iceberg and glacial ice sediments. These data suggest that the net effect of  
352 weathering and atmospheric/cloud processing on these atmospheric dusts has been to produce Fe  
353 (oxyhydr)oxides as the less reactive FeD.. The influence of weathering effects alone on soils  
354 (potential dust precursors) has been studied by Shi et al. (2011), who showed that the ratio



355 (FeA+FeD)/FeT increased from 0.1-0.2 to 0.5-0.6 in highly weathered samples from areas with  
356 relatively high rainfall and temperatures. The (FeA+FeD)/FeT values for the atmospheric dusts  
357 in Table 3 range from 0.24 to 0.52 which are clearly achievable by weathering alone in the  
358 source area. Values of (FeA+FeD)/FeT for the glacial (range 0.013 to 0.059) and iceberg (range  
359 0.063 to 0.201) sediments can also be estimated assuming FeT = 4.2% (mean value for glacial  
360 sediments from Poulton and Raiswell, 2002). These values also suggest a trend of increasing  
361 weathering intensity from the glacial to the iceberg sediments (resulting from ice processing  
362 effects, see earlier) and on to the atmospheric dusts. Further data from atmospheric dusts  
363 delivered to the polar regions are clearly needed to substantiate this conclusion.

### 364 3.5 Atmospheric Dust FeA Fluxes

365 This FeA flux is based on dusts transported through the atmosphere (where there is  
366 potential for cloud processing) and excludes soils. Localised areas of the Ross Sea are subject to  
367 large dust inputs from local terrestrial sands and silts but these appear to be only minor  
368 contributors to productivity (Chewings et al., 2014; Winton et al., 2014). Here we proceed  
369 cautiously on the basis that the FeA content of our atmospheric dusts are representative of those  
370 delivered to the polar regions. Dust deposition fluxes to the SO have been variably estimated as  
371 0.1 to 27 Tg yr<sup>-1</sup> (Gao et al., 2003; Mahowald et al., 2005; Jickells et al., 2005; Li et al., 2008).  
372 The new flux estimates derived here are based on the Community Earth System Model (Albani  
373 et al., 2014), which produces a value of 0.84 Tg yr<sup>-1</sup> for dust deposition to the SO. The model  
374 version we use has been extensively compared to observations, with the sources modified to best  
375 match dust fluxes at high latitude (Albani et al., 2014). In the absence of ice processing,  
376 atmospheric dusts delivered to the SO with an FeA wt. % ranging 0.018 to 0.081% produce a  
377 flux of < 0.01 to 0.01 (mean 0.01) Gmol yr<sup>-1</sup> (Table 5).

378 However the SO is more than 80% covered by sea ice during winter (declining to a  
379 minimum of ~16%) which has residence time of 1-2 years (Vancoppenolle et al., 2013). Studies  
380 of sea ice show that it can be enriched in Fe by up to several orders of magnitude relative to the  
381 underlying seawater and the melting edge is commonly associated with plankton blooms  
382 (Lannuzel et al., 2007; 2008; 2014). This Fe is derived from several sources, including  
383 atmospheric dust deposited on the ice surface (augmented by lithogenic dust in near-shore  
384 regions) and Fe scavenged from seawater during sea ice formation; Vancoppenolle et al., 2013;



385 Wang et al., 2014). Studies of sea ice in Antarctica have shown high concentrations of Fe that  
386 are accompanied by extracellular polymeric substances (EPS) able to solubilise and complex Fe  
387 (Lannuzel et al., 2014). We suggest that atmospheric dust deposited on sea ice is processed by  
388 dissolution (at low pH and aided by EPS) and photoreduction (as described earlier). Our  
389 comparison between glacier and iceberg wt. % FeA contents (Table 3) indicates that this ice  
390 processing has the potential to increase mean wt. % FeA contents by a factor of 2.5 from 0.038  
391 to 0.095 wt. % Simulations with the Community Earth System Model (Albani et al., 2014)  
392 representing the annual cycle of sea ice show that 0.6 Tg yr<sup>-1</sup> of atmospheric dust are deposited  
393 on sea ice that melts (enabling ice processing to occur) which produces a mean rate of FeA  
394 delivery of 0.01 Gmol yr<sup>-1</sup> with a range from <0.01 to 0.02 Gmol yr<sup>-1</sup>. A further 0.24 Tg yr<sup>-1</sup> are  
395 deposited on open water (no ice processing) which supplies only small amounts of FeA (< 0.01  
396 Gmoles yr<sup>-1</sup>). Together the delivery to sea ice and open water supplies a mean of 0.01 Gmol yr<sup>-1</sup>  
397 with a range from <0.01 to 0.03 Gmol yr<sup>-1</sup> (Table 5).

398 New dust Fe flux estimates to the AO (5.1 Tg yr<sup>-1</sup>) are also derived from the Community  
399 Earth System Model (Albani et al., 2014) as before. In the absence of ice processing a mass flux  
400 of 5.1 Tg yr<sup>-1</sup> dust delivers a range of 0.02 to 0.07 (mean 0.03) Gmol yr<sup>-1</sup> of FeA (Table 5). Sea  
401 ice in the Arctic has a maximum extent of < 60% with a residence time of 1-7 years  
402 (Vancoppenolle et al., 2013). That part of the dust flux that falls on sea ice (2.1 Tg yr<sup>-1</sup>) may be  
403 altered by ice processing which increases the wt. % FeA by a factor of 2.5 (see above) before  
404 being released by melting, as with the SO. Ice processed dust delivery to the AO provides a  
405 mean FeA flux of 0.03 Gmol yr<sup>-1</sup> with a range of 0.02 to 0.08 Gmol yr<sup>-1</sup> (Table 5). The 3.0 Tg yr<sup>-1</sup>  
406 of dust delivered to open water supply a mean FeA flux of 0.02 Gmoles yr<sup>-1</sup> (range 0.01 to 0.04  
407 Gmoles yr<sup>-1</sup>) and the total delivery (Table 5) to the AO is the sum of both fluxes (mean 0.05  
408 Gmoles yr<sup>-1</sup>, range 0.03 to 0.12 Gmoles yr<sup>-1</sup>).

#### 409 **4. Discussion and Synthesis**

410 The new iceberg and atmospheric dust data presented here provide a valuable insight into  
411 the iceberg and dust Fe sources to the polar oceans. They substantiate the view that iceberg  
412 sediments have the potential to be a substantial source of bioavailable Fe as ferrihydrite (Table  
413 6). We provide a context for the iceberg sediment flux data by using the global shelf flux value  
414 of Dale et al. (2015) to derive an order of magnitude estimate of shelf sources (thought to be a



415 dominant source in the SO, see earlier). The Arctic and Antarctic shelf areas represent 11.5% and  
416 7.3% of the global shelf area (< 200 m depth; Jahnke, 2010). Combining these area percentages  
417 with the global shelf flux dFe value of 72 Gmol yr<sup>-1</sup> (Dale et al., 2015), suggests shelf sources  
418 are approximately 8.3 Gmol yr<sup>-1</sup> to the AO and 5.3 Gmol yr<sup>-1</sup> to the SO. These values are  
419 numerically comparable to the fluxes from iceberg-hosted sediments although shelf dFe (largely  
420 colloidal or nanoparticulate Fe of unknown composition) and FeA as nanoparticulate ferrihydrite  
421 may not be of similar bioavailability.

422 Sources of variation in Tables 4 and 5 relate both to the estimates of mass fluxes as well as  
423 the Fe analytical data but improved mass flux estimates may be difficult to achieve given their  
424 temporal and spatial variability. Table 6 and Figure 2 summarise the flux ranges. At first sight  
425 there appear to be broad similarities in the magnitude of these Fe sources to the polar oceans but  
426 we list below three limitations to the current data set

- 427 (1) The iceberg FeA fluxes are based on data that is derived mainly from the Arctic.
- 428 (2) The atmospheric dust sample set is small and may not be representative of dusts delivered  
429 to the polar regions.
- 430 (3) FeA is present as ferrihydrite which is potentially bioavailable to phytoplankton although  
431 acquisition rates are unknown and may vary substantially between organisms, and with  
432 local environmental factors (Shaked and Lis, 2012).

433 Iceberg derived FeA is a major source of Fe to both the AO and the SO that will likely  
434 increase as iceberg delivery increases with climate warming in the polar regions (Table 6 and  
435 Figure 2). Our measurements of iceberg FeA contents are based on a substantial data set  
436 although Antarctic data are still poorly represented. It is clear that iceberg FeA is a major source  
437 of potentially bioavailable Fe as ferrihydrite, unless the errors associated with the estimates of  
438 iceberg sediment contents exceed an order of magnitude (Raiswell et al., 2008; Death et al.,  
439 2014; Hawkings et al., 2014). Modelling the impact of iceberg FeA delivery on surface water  
440 dFe concentrations will be complex and will require kinetic models that incorporate scavenging,  
441 complexation, dissolution and sinking (e.g., Tagliabue and Volker, 2011; Raiswell and Canfield,  
442 2012). FeA attached to coarse material will settle out of surface waters quickly, but FeA present  
443 as mainly as fine-grained material (or as nanoparticles) may be held in suspension for long  
444 periods in the wake of icebergs. The basal and sidewall melt from icebergs creates complex



445 patterns of upwelling and turbulence that may last for several weeks and whose influence  
446 extends for tens of km, and from the surface to 200-1500 m depth (Smith et al., 2013).  
447 Furthermore giant icebergs (>18 km in length) have a disproportionally large areal influence  
448 (compared to smaller bergs) which lasts for longer than a month (Luis et al., 2016). The  
449 proportion of the FeA found within this area of influence will clearly have a prolonged residence  
450 time that may be a key factor in its dispersion and utilisation away from iceberg trajectories into  
451 areas with where other Fe supplies are limited.

452 Atmospheric dust fluxes are estimated to be a minor source of FeA to both the AO and  
453 the SO, compared to iceberg-hosted sediment, although substantially larger to the AO (Table 6).  
454 The dust database used here is small but appears to be globally representative in that the range of  
455 wt. % FeD contents (2-5%) overlaps that found in other studies (e.g. Lafon et al., 2004; 2006).  
456 There are no comparable data for potential dust sources to the polar regions although Patagonia  
457 atmospheric dusts (Gaiero et al., 2007) have wt. % total Fe values ranging from 2.9-4.3 wt. %  
458 (which overlaps the 3.5 wt. % total Fe value commonly used as a global average). The important  
459 features of the new FeA and FeD data presented here is that they are closely tied to mineralogy,  
460 with FeA measuring the content of fresh ferrihydrite, which is the most reactive and potentially  
461 bioavailable Fe mineral. Thus these data enable direct comparison with iceberg sediment FeA  
462 delivery. Furthermore we have estimated a potential role for ice processing which appears to  
463 enhance FeA contents of dusts delivered to sea ice. Mean dust FeA concentrations of 0.095 wt.  
464 % (if ice processed) approximate to the mean concentration in icebergs (0.076 wt. %), which  
465 indicates that the former will dominate in areas where dust mass fluxes exceed iceberg sediment  
466 delivery, assuming both types of particulates have similar residence times in the ocean.  
467 Additional atmospheric dust samples from the polar regions are needed to support these cautious  
468 conclusions. Very high soluble Fe contents (Heimbürger et al., 2013) have been found in wet  
469 deposition samples from the Kerguelen Islands (at 48°S which lies outside our SO area) and a  
470 similar flux to the area > 60°S would represent a major contribution.

#### 471 **Acknowledgements**

472 RR thanks the School of Earth and Environment for Greenland fieldwork support and MDK  
473 acknowledges support from the Leverhulme Foundation with grant RPG-406 and LGB from the  
474 UK Natural Environment Research Council grant number NE/J008745/1. JH, MT and JW were  
475 funded by the NERC DELVE project (NERC grant NE/I008845/1 and the associated NERC PhD





476 studentship). The authors are grateful to Lyndsay Hilton from the Thomas Hardy School,  
 477 Dorset, who provided Antarctic glacial ice samples collected during participation on a Fuchs  
 478 Foundation charity expedition. The Patagonian dust samples were supplied by S. Clerici. All the  
 479 data used in this manuscript are included in the Supplementary Information.

480

481

482

483

484

**Table 1.** Comparison of the FeA Content of Different Size Fractions of Iceberg Sediment.

Sample	% FeA
Sieved <1mm	0.175±0.005
Sieved <250 µm	0.172±0.003
Sieved <63 µm	0.162±0.010

**Table 2.** Reproducibility of the <1mm Fraction of Iceberg Sediments.

Sample	% FeA<1mm	% FeA<63 µm
K1	0.374±0.019	0.377
K2	0.094±0.019	0.056
K3	0.044±0.017	0.058
K4	0.129±0.021	0.102
K5	0.089±0.007	0.134



**Table 3.** Composition of Iceberg, Glacial Ice and Atmospheric Dust Samples.

Sample	Wt. %FeA			Wt. %FeD			(FeA+FeD)/FeT
	Low	Mean	High	Low	Mean	High	Estimated Range (see text)
Icebergs (51)	0.03	0.076	0.194	0.20	0.377	0.715	0.063-0.201
Glacial Ice (16)	0.015	0.03	0.060	0.042	0.091	0.196	0.013-0.059
Atmospheric Dust (15)	0.018	0.038	0.081	0.428	0.868	1.76	0.24-0.52

Low and High values each represent one logarithmic standard deviation from the logarithmic mean, except for (FeA+FeD)/FeT.

**Table 4.** Fluxes of FeA Derived from Iceberg-hosted Sediment by Melting.

	Arctic <sup>1</sup>	Antarctic <sup>2</sup>	Sources/Notes
Ice Discharge km <sup>3</sup> yr <sup>-1</sup>	558±55 <sup>a</sup>	1321±144 <sup>b</sup>	a. Bamber et al. (2012) and Van Wychen et al. (2014). b. Depoorter et al (2013).
Sediment Content g litre <sup>-1</sup>	0.5*	0.5*	Estimated by Raiswell et al. (2006), similar to the mean river load.
FeA wt. %	0.03-0.076-0.194	0.03-0.076-0.194	
FeA Flux Gmol yr <sup>-1</sup>	1.4-3.8-11	3.2-9.0-25	

\*Indicates a poorly constrained value.



**Table 5.** Atmospheric Dust FeA Fluxes

	Arctic	Antarctic	Sources/Notes
Mass Flux Tg yr <sup>-1</sup>	5.1	0.84	Community Earth Systems Model (Albani et al., 2014)
FeA wt. % (No ice processing)	0.018-0.038-0.081*	0.018-0.038-0.081*	Based on 15 dust samples from the Atlantic, Mediterranean and Patagonia.
FeA Flux Gmol yr <sup>-1</sup>	0.02-0.03-0.07	<0.01-0.01-0.01	
FeA wt. % (With ice processing)	0.045-0.095-0.203*	0.045-0.095-0.203*	Assuming ice processing increases concentrations by 2.5x
FeA Flux Gmol yr <sup>-1</sup>	0.03-0.05-0.12	<0.01-0.01-0.03	

\*Indicates poorly constrained values

**Table 6.** Summary Data for the Main Sources of Iron to the Arctic and Southern Oceans

Source	FeA flux range Gmol yr <sup>-1</sup>	
	Arctic Ocean	Southern Ocean
<i>Iceberg Sediments</i>	1.4 – 11	3.2 – 25
<i>Atmospheric dust</i>	0.05 – 0.19	0.01 – 0.05
Ice processed	0.03 – 0.12	<0.01 – 0.03
No ice processing	0.02 – 0.07	<0.01 – 0.02



486

487 Figure 1. Simplified reaction scheme for the reactions of ice-hosted sediments during  
 488 melting/freezing cycles.

489

490

491

492

493

494

495

496

497

498

499

500

501

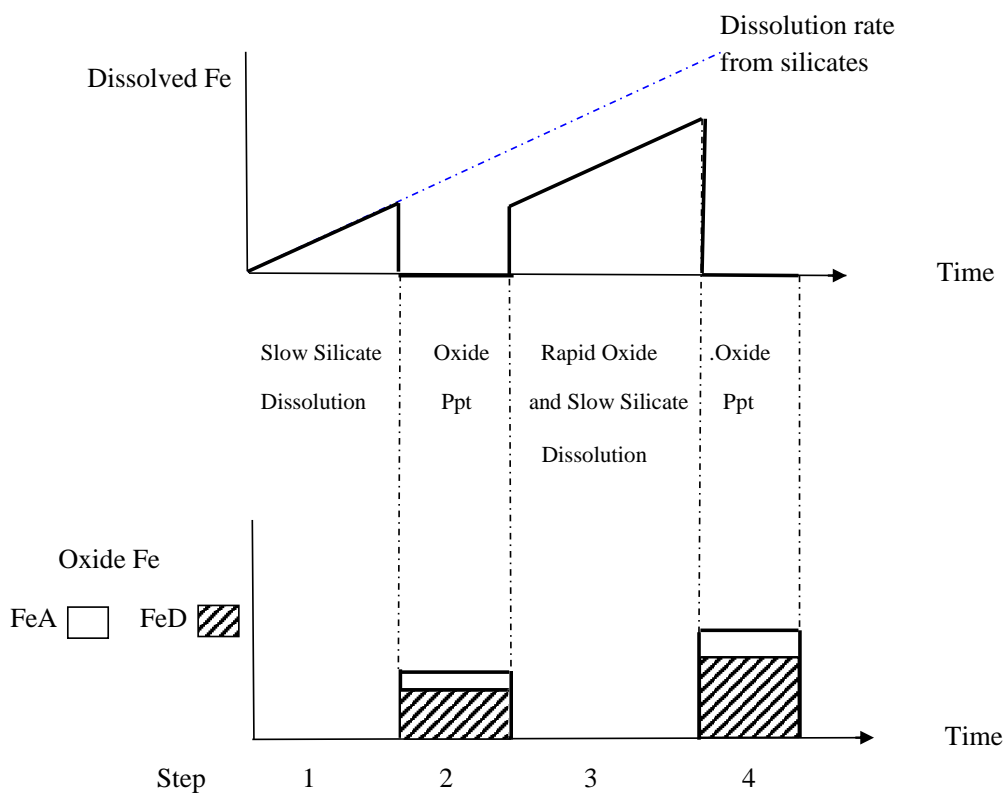
502

503

504

505

506

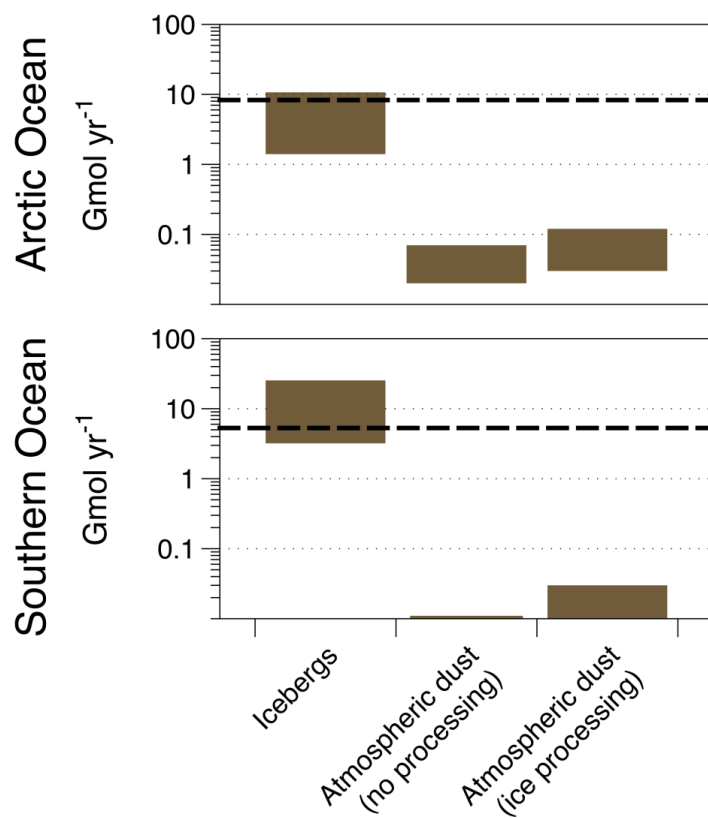




507

508 Figure 2. Ranges of FeA fluxes to the Arctic and Southern Oceans. Dashed line shows rough  
509 estimates of shelf dFe based on Dale et al. (2015).

510



511

512

513

514

515



## 516 **References**

- 517 Albani, S., Mahowald, N. M., Perry, A. T., Scanza, R. A., Zender, C. S., Heavens, N. G., Maggi,  
518 V., Kok, J. F., and Otto-Bliesner, B. L.; Improved dust representation in the Community  
519 Atmosphere Model, *J. Adv. Model. Earth Syst.*, 6, 541–570, doi:10.1002/2013MS000279, 2014.
- 520 Baker, A.R., Jickells, T.D., Witt, M., and Linge, K.L.; Trends in the solubility of iron,  
521 aluminium, manganese and phosphorus in aerosol collected over the Atlantic Ocean, *Mar.*  
522 *Chem.*, 98, 43-58, 2006.
- 523 Baker, A.R., and Croot, P.L.; Atmospheric and marine controls on aerosol solubility in seawater,  
524 *Mar. Chem.*, 120, 4-13, 2010.
- 525 Bamber, J., van den Broeke, M., Ettema, J., Lenarts, J., and Rignot, E.; Recent large increases  
526 in freshwater fluxes from Greenland into the North Atlantic, *Geophys. Res. Lett.*, 39, L19501,  
527 doi:10.1029/2012/GL050552, 2012.
- 528 Benning, L.G., A. M. Arieso, A.M., Lutz, S., and Tranter, M.; Biological impact on Greenland's  
529 albedo, *Nat. Geosci.*, 7, 691, 2014. Boyd, P.W., Arrigo, K.R., Stzepekand, R., and van Dijken,  
530 G.L.; Mapping phytoplankton iron utilization: insights into Southern Ocean supply mechanisms,  
531 *J. Geophys. Res.*, 117, doi:org/10.1029/2011JC00726, 2012.
- 532 Boyd, P.W., Mackie, D.S., and Hunter, K.A.; Aerosol iron deposition to the surface ocean-  
533 Modes of iron supply and biological responses, *Mar. Chem.*, 120, 128-143, 2010.
- 534 Breitbarth, E., E.P. Achterberg, E.P., Ardelan, M.V., Baker, A.R., Bucciarelli, E., Chever, F.,  
535 Croot, P.L., Duggen, S., Gledhill, M., Hasselhov, M., Hassler, C., Hoffmann, L.J., Hunter, K.A.,  
536 Hutchins, D.A., Ingri, J., Jickells, T., Lohan, M.C., Nielsdottir, M.C., G. Sarthou, G.,  
537 Schoemann, V., Trapp, J.M., Turner, D.R., and Ye, Y.; Iron biogeochemistry across marine  
538 systems-progress from the past decade, *Biogeosciences*, 7, 1075-1095, 2010, 2010.
- 539 Brinza, L.; Interactions of molybdenum and vanadium and iron nanoparticles, PhD thesis,  
540 University of Leeds, 2010.
- 541 Chen, Y., and R.L. Siefert, R.L.; Determination of different types of labile atmospheric iron over  
542 remote oceans, *J. Geophys. Res.*, 108, D24, 4774, doi:1029/2003JD003515, 2003.



- 543 Chewings, J.M., Atkins, C.B. Dunbar, G.B., and Golledge, N.R.; Aeolian sediment transport and  
544 deposition in a modern high-latitude glacial marine environment, *Sedimentology*, 61, 1535-1557,  
545 2014.
- 546 Conway, T.M., Wolf, E.W., Rothlisberger, R., Mulvaney, R., and Elderfield, H.E.; Constraints  
547 on soluble aerosol iron flux to the southern Ocean during the Last Glacial Maximum, *Nat.*  
548 *Comms.*, 6:7850 doi:10.1038/ncomms8850, 2015.
- 549 Dale, A.W., Nickelsen, L., Scholz, F., Hensen, C., Oschlies, A., and Wallman, K.; A revised  
550 global estimate of dissolved iron fluxes from marine sediments, *Global Biogeochem. Cycles*,  
551 doi:10.1002/2014GB005017, 2015.
- 552 Death, R., Wadham, J.L., Monteiro, F., Le Brocq, A.M., Tranter, M., Ridgwell, A.,  
553 Dutkiewicz, S., and Raiswell, R.; Antarctic ice sheet fertilizes the Southern Ocean,  
554 *Biogeosciences*, 10, 12551-12570, 2014..
- 555 Depoorter, M.A., Bamber, G.L., Griggs, J.A.T.M. Lenaerts, T.M., Ligtenberg, S.R.M., van den  
556 Broeke, M.R., and Moholdt, G.; Calving fluxes and basal melt rates of Antarctic ice shelves,  
557 *Nature*, 502, 89-92, 2013, 2013.
- 558 Gaiero, D.M., Brunet, F., Probst, J-L., and Depetris, P. J.; A uniform isotopic and chemical  
559 signature of dust exported from Patagonia: Rock sources and occurrence in southern  
560 environments, *Chem. Geol.*, 238, 107-129, 2007.
- 561 Gao, Y., Fan, S-M., and Sarmiento, J.L.; Atmospheric iron input to the ocean through  
562 precipitation scavenging: a modeling perspective and its implication for natural iron fertilization  
563 in the ocean, *J. Geophys. Res.*, 108, 4221, doi:10.1029/2002/JD002420, 2003.
- 564 Hawkings, J.R., Wadham, J.L., M. Tranter, M., Raiswell, R., Benning, L.G., Statham, P.J., A.  
565 Tedstone, A., Nienow, P., Lee, K., and J. Telling, J.; Ice sheets as a significant source of  
566 highly reactive nanoparticulate iron to the oceans, *Nat. Comms.*, 5.3929,  
567 doi:10.1038/ncomms4929, 2014.



- 568 Heimburger, A., Lusno, R., and S. Triquet, S.; Solubility of iron and other trace elements in  
569 rainwater collected on the Kerguelen Islands (South Indian Ocean), *Biogeosciences*, 10, 6616-  
570 6628, 2013.
- 571 Hopwood, M.J., Statham, P.J., Tranter, M., and Wadham, J.L.; Glacial flours as a potential  
572 source of Fe(II) and Fe(III) to polar waters, *Biogeochemistry*, doi:10.1007/s10533-013-9945-y,  
573 2014.
- 574 Hyacinthe, C., and Van Cappellen, P.; An authigenic iron phosphate phase in estuarine  
575 sediments: composition, formation and chemical reactivity, *Mar. Chem.*, 91, 227-251, 2004.
- 576 IPCC; Long-term Climate Change: Projections, Commitments and Irreversibility, 5 th  
577 Assessment Report, Chapter 12, 2013.
- 578 Jahnke, R.A.; Global Synthesis in Carbon and Nutrient Fluxes in Continental Margins, *Global*  
579 *Change-The IGBP Series*, edited by Liu K.-K et al., Chapter 16. Springer-Verlag, Berlin, 2010.
- 580 Jickells, T.D., and Spokes, L.J.; Atmospheric inputs to the ocean, in *The Biogeochemistry of*  
581 *Iron in Seawater*, edited by D.R. Turner and K.A. Hunter, pp.123-251. Wiley, New York, 2001.
- 582 Jickells, T.D., An, Z.S., Anderson, K.K., Baker, A.R., Bergametti, G., Brooks, N., Cao, J.J.,  
583 Boyd, P.W., Duce, R.A., Hunter, K.A., Kawaahata, H., Kubilay, N., LaRoche, J., J., Liss, P.S.,  
584 Mahowald, N., Prospero, J.M., Ridgwell, A., Tegen, I., and Torres, R.; Global iron connections  
585 between desert dust, ocean biogeochemistry, and climate, *Science*, 308, 67-73., 2005.
- 586 Kim, K., Choi, W., Hoffmann, M.R., Yoon, H.I., and Park B.K.; Photoreductive dissolution of  
587 iron oxides trapped in ice and its environmental implications, *Env. Sci., Tech.*, 44, 4142-4148,  
588 2010.
- 589 Kostka, J.E., and Luther III, G.W.; Partitioning and speciation of solid phase iron in saltmarsh  
590 sediments, *Geochim. Cosmochim. Acta*, 58, 1701-1710, 1994.
- 591 Kuma, K., and Matsunaga, K.; Availability of colloidal ferric oxides to coastal marine  
592 phytoplankton, *Mar. Biol.*, 122, 1-11, 1995.





- 593 Lafon, S., Rajot, J-L., Alfaro, S.C. and Gaudichet, S.; Quantification of iron oxides in desert  
594 aerosol, *Atmos. Env.*, 38, 1211-1218, 2004.
- 595 Lafon, S., Sokolik, I.N., Rajot, J-L., Caquineau, S., and Gaudichet, S.; Characterization of iron  
596 oxides in mineral dust aerosols; implications for light absorption, *J. Geophys.Res.*, 111, D21207,  
597 2006.
- 598 Lancelot, C., de Montey, A., Goose, H., Becquefort, S., Schoemann, V., Basquer, B., and  
599 Vancoppenolle, M.; Spatial distribution of the iron supply to phytoplankton in the Southern  
600 Ocean: a model study, *Biogeosciences*, 6, 2861-2878, 2009.
- 601 Lannuzel, D., Schoemann, V., de Jong, J., Tison, J-L., and Chou, L. (2007), Distribution and  
602 biogeochemical behavior of iron in the East Antarctic sea ice, *Mar.Chem*, 106, 18-32, 2007.
- 603 Lannuzel, D., Schoemann, V., de Jong, J., Chou, L., Delille, B., Becquevort, S., and Tison, J-L.;  
604 Iron study in during a time series in the western Weddell Sea pack ice, *Mar. Chem.*, 108, 85-95,  
605 2008.
- 606 Lannuzel, D., van der Merwe, P.C., Townsend, A.T., and Bowie, A.R.;Size fractionation of  
607 iron, manganese and aluminium in Antarctic fast ice reveals a lithogenic origin and low iron  
608 solubility, *Mar. Chem.*, 161, 47-56, 2014.
- 609 Li, F., Ginoux, P., and V. Ramaswamy, V.; Distribution, transport, and deposition of mineral  
610 dust in the Southern Ocean and Antarctica: contribution of major sources, *J. Geophys. Res.*, 113,  
611 D10207, doi:10.1029/2007JD009190, 2008.
- 612 Lin, H., and Twining, B.S.; Chemical speciation of iron in Antarctic waters surrounding free-  
613 drifting icebergs, *Mar. Chem.*, 128-129, 81-91, 2012.
- 614 Luis, P., Duprat, A.M., Bigg, G.R., and Wilton, D.J.; Giant icebergs significantly enhance the  
615 marine productivity of the Southern Ocean, *Nat. Geosci*, doi.10.1038NGEO2533, 2016.
- 616 Luo, C., Mahowald, N., Bond, T., Chuang, P.Y., Artaxo, P., Siefert, R., Chen, Y., and J.  
617 Schauer, J.; Combustion iron distribution and deposition, *Global Biogeochem.Cycles*, 22,  
618 GB1012, 2008..



- 619 Lutz, A.M., Arieso, S.E., Villar, J., and Benning, L.G.; Variation in algal communities cause  
620 darkening of a Greenland glacier, F.E.M.S., *Microbial Ecol.*, 89, 402-414, 2014.
- 621 Mackenzie, F.T., and Andersson, A.J.; The marine carbon cycle and ocean acidification during  
622 Phanerozoic time, *Geochem. Perspect.*, 2, 1-227, 2013.
- 623 Mahowald, N., Baker, A., Bergametti, G., Brooks, N., Duce, R., Jickells, T.D., Kubilay, N.,  
624 Prospero, J., and Tegen, I.; The atmospheric global dust cycle and iron inputs into the ocean, *J.*  
625 *Geophys. Res.*, 111, D05303, doi:10.1029/2005JD006459, 2005.
- 626 Meguro, H., Toba, Y., Murakami, H., and Kimura, N.; Simultaneous remote sensing of  
627 chlorophyll, sea ice and sea surface temperature in the Antarctic waters with special reference to  
628 the primary production from ice algae, *Adv. Space Res.*, 33, 116-1172, 2004.
- 629 Moore, C.M., Mills, M.M., Arrigo, K.R., Berman-Frank, I., Boyd, P.W., E.D. Galbraith, E.D.,  
630 Geidler, R.J., Guieu, C., Jaccard, S.L., Jickells, T.D., La Roche, J., Lenton, T.M., Mahowald,  
631 N.M., Marnon, E., Marinov, I., Moore, J.K., Nakatsuka, T., Oschlies, A., Saito, M.A., Thingstad,  
632 T.F., Tsuda, A., and Ulloa, O.; Processes and patterns of oceanic nutrient limitation, *Nat.*  
633 *Geosci.*, 6, 701-710, 2013.
- 634 Moore, J.K., Abbott, M.R., and J.G. Richman (1999), Location and dynamics of the Antarctic  
635 Polar Front from satellite sea surface temperature data, *J. Geophys. Res.*, 104, 3059-3073, 1999.
- 636 Nielsdottir, M.C., Moore, C.M., Sanders, R., Hinz D.J., and Achterberg, E.P.; Iron limitation of  
637 the postbloom phytoplankton communities in the Iceland Basin. *Global Biogeochem.Cycles*, 23,  
638 GB3001, 2009.
- 639 Nodwell, L.M., and Price, N.M.; Direct use of inorganic colloidal iron by marine thixotrophic  
640 phytoplankton, *Limnol. Oceanog.*, 46, 765-777, 2001.
- 641 Pabi, S., van Dijken, G.L., and Arrigo, K.R.; Primary production in the Arctic Ocean, *J.*  
642 *Geophys. Res.*, **113**, C08005, doi.org/10.1029/2007JC004578, 2008.



- 643 Popova, E. E., Yool, A., Coward, A.C., Aksenov, Y.K., Alderson, S.G., de Cuevas, B.A., and  
644 Anderson, T.F.; Control of primary production in the Arctic by nutrients and light: insights from  
645 a high resolution ocean general circulation model, *Biogeosciences*, 7, 3569-3591, 2010.
- 646 Poulton, S.W., and Canfield, D.E.; Development of a sequential extraction procedure for iron:  
647 implications for iron partitioning in continentally-derived particulates, *Chem. Geol.*, 214, 209-  
648 221, 2005.
- 649 Poulton S.W., and Raiswell, R.; The low-temperature geochemical cycle of iron: from  
650 continental fluxes to marine sediment deposition, *Amer. J. Sci.*, 302, 774-805, 2002.
- 651 Pritchard, H.D., Ligtenberg, S.R.M., Fricker, H.A., Vaughan, D.G., van den Broeke, M.R., and  
652 L. Padman, L.; Antarctic ice-sheet loss driven by basal melting, *Nature*, 484, 502-505, 2012.
- 653 Raiswell, R.; Iceberg-hosted nanoparticulate Fe in the Southern Ocean: Mineralogy, origin,  
654 dissolution kinetics and source of bioavailable Fe, *Deep-Sea Res. II*, 58, 1364-1375, 2011.
- 655 Raiswell, R., and Canfield, D.E.; The iron biogeochemical cycle past and present, *Geochem.*  
656 *Perspect.*, 1, 1-220, 2012.
- 657 Raiswell, R., Canfield, D.E., and Berner, R.A.; A comparison of iron extraction methods for the  
658 determination of degree of pyritization and recognition of iron-limited pyrite formation, *Chem.*  
659 *Geol.*, **111**, 101-111, 1994.
- 660 Raiswell R., Tranter, M., Benning, L.G., Siegert, M., Death, R., Huybrechts, R.P., and T. Payne,  
661 T.; Contributions from glacially derived sediment to the global iron oxyhydroxide cycle:  
662 implications for iron delivery to the oceans, *Geochim. Cosmochim. Acta*, 70, 2765-2780, 2006.
- 663 Raiswell, R., Benning, L.G., Tranter, M., and Tulaczyk, S.; Bioavailable iron in the Southern  
664 Ocean: The significance of the iceberg conveyor belt, *Geochem. Trans.* 9, doi:10.1186/1467-  
665 4866-9-7, 2008.
- 666 Raiswell, R., Vu, H.P., Brinza, L., and Benning, L.G.; The determination of Fe in ferrihydrite by  
667 ascorbic acid extraction: methodology, dissolution kinetics and loss of solubility with age and  
668 de-watering, *Chem. Geol.*, 278, 70-79, 2010.



- 669 Rich H.W., and Morel, F.M.M.; Availability of well-defined iron colloids to the marine diatom  
670 *Thalassiosira weissflogii*, *Limnol. Oceanog.*, 35, 652-662, 1990.
- 671 Rignot, E., Velicogna, I., van den Broeke, M.R., Monaghan, A., and Lenaerts, J.; Acceleration  
672 of the contribution of the Greenland and Antarctic ice sheets to sea level rise, *Geophys. Res.*  
673 *Let.*, 38, L05503, 2011.
- 674 Schulz, M., Prospero, J.M., Baker, A.R., Dentener, F., Ickes, L., Liss, P.S., Mahowald, N.,  
675 Nickovic, S., Garcia-Pando, C.P., Rodriguez, S., Sarin, M., Tegen, I., and Duce, R.A.;  
676 Atmospheric transport and deposition of mineral dust to the ocean: implications for research  
677 needs, *Env. Sci. Tech.*, 46, 10390-10404, 2012.
- 678 Schwertmann, U., Stanjek, H., and Becher, H.-H.; Long term in vitro transformation of 2-line  
679 ferrihydrite to goethite/hematite at 4, 10, 15 and 25°C, *Clay Minerals*, 39, 433-438, 2004.
- 680 Shaked, Y., and Lis, H.; Disassembling iron availability to phytoplankton, *Front. Microbiol.*,  
681 123, 1-26, 2012.
- 682 Shaw, T.J., Raiswell, R., Hexel, C.R., Vu, H.P., Moore, W.S., Dudgeon, R., Smith, K.L.; Input,  
683 composition and potential impact of terrigenous material from free-drifting icebergs in the  
684 Weddell Sea, *Deep-Sea Res. II*, 58, 1376-1383, 2011.
- 685 Shi, Z., Krom, M.D., Bonneville, S., Baker, A.R., Bristow, C., Mann, G., Carslaw, K.,  
686 McQuaid, J.B., Jickells, T., and L.G. Benning, L.G.; Influence of chemical weathering and aging  
687 of iron oxides on the potential iron solubility of Saharan dust during simulated atmospheric  
688 processing, *Global Biogeochem. Cycles*, 25, GB2010, doi:10.1029/2010GBC003837, 2011.
- 689 Shi, Z., Krom, M.D., Jickells, T.D., Bonneville, S., Carslaw, K.S., Mihalpoulos, N., Baker, A.R.,  
690 and Benning, L.G.; Impacts on iron solubility in the mineral dust by processes in the source  
691 region and the atmosphere: a review, *Aeolian. Res.*, 5, 21-42, 2012.
- 692 Smith, K.L., Robison, B.H., Helly, J.J., Kaufmann, R.S., Ruhl, H.A., Shaw, T.J., Twining, B.S.,  
693 and Vernat, M.; Free-drifting icebergs: Hot spots of chemical and biological enrichment in the  
694 Weddell Sea, *Science*, 317, 478-483, 2007.



- 695 Smith, K.L. Jr., Sherman, A.D., Shaw, T.J., and Springall, J.; Icebergs as unique Lagrangian  
696 ecosystems in polar seas, *Ann. Rev. Mar. Sci.*, 5, 269-287, 2013.
- 697 Stookey, L.L.; Ferrozine- a new spectrophotometric reagent for iron, *Anal. Chem.*, 42, 779-781,  
698 1980.
- 699 Sugie, K., Nishioka, J., Kuma, K., Volkov, Y.N., and Nataksuka, T.; Availability of particulate  
700 Fe to phytoplankton in the Sea of Okhotsk, *Mar. Chem.*, 152, 20-31, 2013.
- 701 Tagliabue, A., Bopp, L., and Aumont, O.; Evaluating the importance of atmospheric and  
702 sedimentary iron sources to Southern Ocean biogeochemistry, *Geophys. Res. Lett.*, 36, L13601,  
703 doi:10.1029/2009GL038914, 2009.
- 704 Tagliabue, A., Bopp, L., Dupay, J-C., Bowie, A.R., Chever, F., Jean-Bapiste, P., Bucciarelli, E.,  
705 Lannuzel, D., Remenyi, T., Sarthou, G., Aumont, O., Gehlen, M., and Jeandel, C.; Hydrothermal  
706 contribution to the oceanic inventory, *Nature Geosci.*, 3, 252-256, 2010.
- 707 Tagliabue, A., and Volker, C., Towards accounting for dissolved iron speciation in global ocean  
708 models, *Biogeosciences*, 8, 3025-3039, 2011.
- 709 Tagliabue, A., Aumont, O., Death, R., Dunne, J.P., Dutkiewicz, S., Galbraith, E., Misumi, K.,  
710 Moore, J.K., Ridgwell, A., Sherman, E., Stock, C., Vichi, M., Volker, C., and Yool, A.; How  
711 well do global ocean biogeochemistry models simulate dissolved iron distributions? *Global*  
712 *Biogeochem. Cycles*, doi:10.1002/2015GB005289.
- 713 Tranter, M., and Jones, H.G.; The chemistry of snow: processes and nutrient recycling, in *The*  
714 *Ecology of Snow*, edited by H.G. Jones, J.W. Pomeroy, D.A. Walker, and R. Hoham, pp. 127-  
715 167, Cambridge University Press, 2001.
- 716 Vancoppenolle, M., Meiners, K.M., Michel, C., Bopp, L., Brabant, F., Carnat, G., Delille, B.,  
717 Lannuzel, D., Madec, G., Moreau, S., Tison, J-L., and van der Merwe, P.; Role of sea ice in  
718 global biogeochemical cycles: emerging views and challenges, *Quat. Sci. Reviews*, 79, 207-230,  
719 2013.



- 720 Van Wychen, W., Burgess, D.O., Gray, L., Copland, L., Sharp, M., Dowdeswell, J.A., and  
721 Bentham, T.J.; Glacier velocities and dynamic ice discharge from the Queen Elizabeth Islands,  
722 Nunavut, Canada. *Geophys. Res. Lett*, 41, doi 19:1002/2013GL058558.
- 723 Vaughan, D.G.; Recent trends in melting conditions on the Antarctic Peninsula and their  
724 implications for ice-sheet mass balance and sea level, *Arctic Ant. Alpine Res.*, 38, 147-152,  
725 2006.
- 726 Wadley, M.R. Jickells, T.D., and Heywood, K.J.; The role of iron sources and transport for  
727 Southern Ocean productivity, *Deep-Sea Res. I*, 87, 82-94, 2014.
- 728 Wang, S., Bailey, D., Lindsay, K., Moore, J.K., and Holland, M.; Impact of sea ice on the marine  
729 iron cycle and phytoplankton productivity, *Biogeosciences*, 11, 4713-4731, 2014.
- 730 Wells, M.L., Zorkin, N.G., and Lewis, A.G.; The role of colloid chemistry in providing a source  
731 of iron to phytoplankton. *J. Mar. Res.*, 41, 731-746, 1983.
- 732 Winton, V.H.L., Dunbar, G.B., Berteler, N.A.N., Millet, M-A., Delmonte, B., Atkins, C.B.,  
733 Chewings J.M., and Andersson, P.; The contribution of aeolian sand and dust to iron fertilization  
734 of phytoplankton blooms in the southwestern Ross Sea, Antarctica, *Global Biogeochem. Cycles*,  
735 28, 423–436, doi: 10.1002/2013GB004574, 2014.
- 736
- 737
- 738